

Polarization beam splitter based on a photonic crystal heterostructure

E. Schonbrun, Q. Wu, and W. Park

Department of Electrical Engineering, University of Colorado at Boulder, Boulder, Colorado 80309-0425

T. Yamashita and C. J. Summers

Department of Material Science and Engineering, Georgia Institute of Technology, Atlanta, Georgia 30332-0245

Received May 31, 2006; accepted August 4, 2006;
 posted August 16, 2006 (Doc. ID 71543); published October 11, 2006

The design and characterization of a photonic crystal (PC) polarization beam splitter (PBS) that operates with an extinction ratio of greater than 15 dB for both polarizations are presented. The PBS is fabricated on a silicon-on-insulator (SOI) wafer where the input and output ports consist of 5 μm wide ridge waveguides. A large spectral shift is observed in the dispersion plots of the lowest-order even (TE-like) and odd (TM-like) modes due to the SOI confinement. Because of this shift, the TE-like mode is close to a directional gap at the top of the band, and the TM-like mode is in a low-frequency regime where the dispersion surface is almost isotropic. We show that the TE-like mode has very high reflection at the interface between the two PCs, whereas the TM-like mode exhibits a very high transmission. © 2006 Optical Society of America
OCIS codes: 130.3120, 230.5440, 230.7400.

Slab photonic crystals (PCs) are becoming increasingly important in the field of semiconductor integrated optics.^{1,2} The ability to incorporate several different optical functions on a single chip, preferably silicon, is powerful because this represents a complete integration of optical devices with silicon electronics. To do this, however, silicon needs to take on a variety of different optical properties to perform the various needed functionalities. PC structure provides an effective means to engineer the dispersion surfaces to meet the specific needs of a given application.³⁻⁵ In this Letter, we take advantage of the fact that, due to the large index contrast, silicon-based PCs can have anomalous dispersion over a large bandwidth. Using this unique characteristic, we design and demonstrate a broad bandwidth polarization beam splitter (PBS) that works based on the induced birefringence and anisotropy of a slab PC.

Because of the inherent anisotropy of a 2D periodic structure, 2D PCs have a polarization-dependent response. Two different schemes have been reported to use 2D PC structures to split different incident polarization states. The first is to use the superprism effect.⁶ With this method, incident beams with different polarization states refract at different angles due to the polarization-dependent anisotropy of the photonic band structure. High extinction ratios could be obtained with this technique, but this comes at the expense of a small operational bandwidth and an extended PC region to obtain the needed beam separation. A second method is to use the spectral shift found in the lowest photonic bandgap for TE and TM modes to make a polarization sensitive reflector.^{7,8} This scheme has the benefit of being rectilinear and can be made much smaller, but it is difficult to obtain large extinction ratios because there is usually a non-negligible reflection. Traditional crystal PBSs are cut at the Brewster angle so this reflection can be made small, but to the best of our knowledge, this effect

has not been found in PCs. In our device, this reflection occurs at the interface between two PCs with different lattice constants but the same fill factor. In the long wavelength regime where light sees an averaged index proportional to the fill factor, reflection at this interface can be very small. In our device, this is the case for the TM mode, which lies well below the band edge. In contrast, the strong confinement of the silicon slab spectrally shifts the TE mode up close to the band edge, putting it in a highly reflective region. We take advantage of these two effects to create a PBS that has the benefits of a reflection geometry, small size, and the capability of large extinction ratios.

There is a large birefringence in a thin SOI wafer based on the effective index of the two lowest-order guided modes. In this Letter, we refer to modes in SOI wafers as even (TE-like) and odd (TM-like) in reference to the mirror symmetry of the magnetic field component perpendicular to the device layer. Strictly speaking, our structure does not have mirror symmetry perpendicular to the substrate. However, the mode profiles have a strong resemblance to strictly even and odd modes due to the large index contrast both above and below the device layer. In the PC region, in addition to the background slab birefringence, the periodicity of the structure leads to directional gaps above the first band. The combination of these two effects leads to a total response of the system where one polarization is reflected, because it is within the directional gap, and the other polarization is transmitted across the PC interface, because it lies solidly in the first photonic band. Both the device layer thickness, which affects the intrinsic birefringence, and the PC lattice parameters, which determine the location of the directional gaps, have been carefully engineered in this system.

As shown in Fig. 1, the geometry of the device is similar to a traditional cube beam splitter. A square-shaped PC region is separated along the diagonal

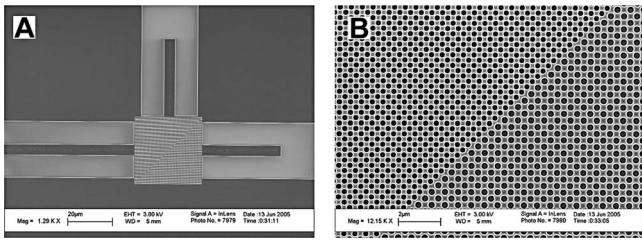


Fig. 1. A, Scanning electron micrograph (SEM) of the integrated PC PBS device with input (left) and output (top and right) $5\ \mu\text{m}$ wide ridge waveguides. B, Higher magnification SEM image of the interface between the two PCs. The first (left) PC has a lattice constant of $353\ \text{nm}$, and the second (right) PC has a lattice constant of $438\ \text{nm}$, and both have the same radius to lattice constant ratio of 0.35 . The dark regions in A consist of a $300\ \text{nm}$ thick silicon layer, and the bright regions are where the device layer has been etched down to the underlying $1\ \mu\text{m}$ oxide.

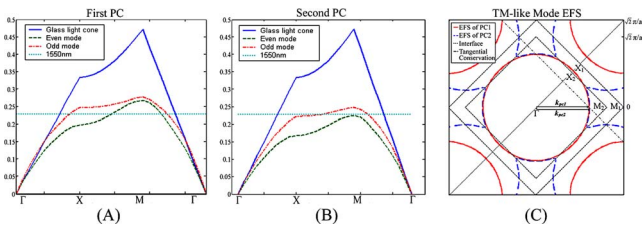


Fig. 2. (Color online) (A) and (B) show the first photonic bands and the light line for the first and second PC, respectively. Due to the proximity to the band edge, there is no coupling from the first PC to the second for the TE-like mode, whereas TM-like mode coupling is shown in (C) for $1550\ \text{nm}$ light.

into two different PCs that are linearly scaled versions of each other. The first PC located on the left side of the heterostructure has a lattice constant that is smaller by a factor of 0.806 than the second PC placed on the right side of the heterointerface. Both PCs are composed of a square array of air holes with the same radius to the lattice constant ratio of 0.35 and the same crystal orientation. The PCs are oriented such that the vertical and horizontal interfaces are along the $\langle 11 \rangle$ direction, and the diagonal interface is along the $\langle 10 \rangle$ direction. At the diagonal interface, the PC modes must have their transverse momentum matched across this boundary in order to be transmitted. There is a range of frequencies below the ΓM band edge and above the X point where the tangential momentum boundary conditions are not satisfied. Unlike a bandgap reflector, the location and the shape of the first photonic band are critical.

Figure 2 shows the photonic band structures in both the first [Fig. 2(A)] and the second PC [Fig. 2(B)] regions for TE- and TM-like modes calculated by using the plane-wave method with a 3D supercell.⁹ To make direct comparisons between the two PC structures, all frequencies are represented in the units of $2\pi c/a_1$ where a_1 is the lattice constant of the first PC. As a result, the band structure of the second PC is scaled by 0.806 , which is the ratio of lattice constants in the two PC regions. For the second PC, the band edge occurs at ω_n ($\omega a_1/2\pi c$) = 0.225 and 0.248 for the TE- and TM-like modes, respectively, and is located

at the M point of the first Brillouin zone. If light were normally incident into the PC in the ΓM direction, these frequency values would represent the spectral cutoffs for transmission into the second PC, and the device would act as an effective PBS at frequencies in between these cutoffs. In our device, light is incident at a 45° angle with respect to the normal of the second PC, so not only must there be a mode at this frequency, but it also has to be able to match its transverse momentum across the boundary. In effect, this decreases the cutoff frequency for transmission to 0.219 and 0.245 for TE- and TM-like modes, respectively. The matching of the TM-like mode across the boundary to the two PCs is shown in Fig. 2(C). Since the second PC has a larger lattice constant, the Brillouin zone is smaller and the consequent band folding introduces a directional gap along the ΓX direction. Along the ΓM direction, the equifrequency surface of the second PC closely overlaps that of the first PC, because the two PCs have the same fill factor. Consequently, the magnitude of the momentum vector is matched very well across the boundary so the two TM-like Bloch modes couple efficiently to each other.

The response of the device was characterized from 1520 to $1605\ \text{nm}$ or $\omega_n = 0.220$ to 0.232 . For this entire bandwidth, the TE-like mode is near the region of self-collimation¹⁰ in the first PC and close or above the band edge in the second PC. Consequently, there is very high reflection at the interface. Furthermore, the beam is self-collimated with very little diffraction before and after the reflection, and the field profile incident on the reflected output port waveguide matches well with the field leaving the incident waveguide as shown in Fig. 3(B). On the other hand, the TM-like mode efficiently couples across the PC interface as shown in Fig. 3(A). In the second PC, the TM-like mode is also close to the self-collimation regime, but the EFS still has some positive curvature with respect to the Γ point as shown in Fig. 2(C). The field therefore positively diffracts as it propagates through the first and second PC and does not couple into the output waveguide as well as the TE-like mode. This can be seen in Fig. 3(A) by the increased scatter in the vicinity of the output port waveguide.

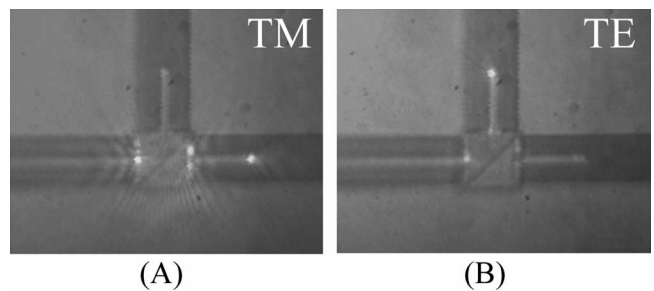


Fig. 3. Images show out-of-plane scattered light collected over the device at $1582\ \text{nm}$. From the scattered intensity it is clear that when illuminated with TM light the transmitted port is bright, and when illuminated with TE light the reflected port is bright. The polarization of the incident light is controlled with a polarization controlling paddle and coupled into the device via a fiber-coupled laser. The device is illuminated by a lamp to show its geometry.

For both polarizations, there occurs very low scatter at the heterointerface, demonstrating its low loss functionality.

Because the vidicon camera response is not linear, extinction ratios of the two ports were measured with an InGaAs photodiode. We used a pinhole to aperture the scattered field and filter out all the light except for that leaving the termination of the port of interest. The power levels could then be accurately measured from each port under illumination with TE and TM light. Extinction ratios are calculated with the expression $\text{dB} = 10 \log_{10} P_{p1}/P_{p2}$, where P_{p1} is the power in the primary polarization for the port, and P_{p2} is the power in the cross polarization for the port. At a wavelength of 1582 nm, the response for both ports is the best at 15.7 and 16.5 dB for the reflected port and the transmitted port, respectively. In the characterized wavelength range, the best reflection port extinction ratio is 17.9 dB, and the best transmission port extinction ratio is 19.7 dB at 1600 and 1528 nm, respectively. This follows the general trend where the performance of the reflection port deteriorates with increasing frequency, as the TM-like mode is increasingly reflected, and the performance of the transmission port improves with increasing frequency, as the TE-like mode has decreasing transmission.

In conclusion, a reflection-geometry PC PBS with high extinction ratios is presented that separates an incident beam into its TE- and TM-like polarization components based on the polarization-dependent coupling from one PC to another. The device utilizes a novel mechanism for obtaining high TM-like mode transmission based on the coupling through two PCs with different lattice constants but the same fill factor. The TE-like polarization exhibits high reflection due to the photonic bandgap and is efficiently collected in the reflection port as it is routed through the

PC in the self-collimation regime. This device shows that slab photonic crystal circuits made out of silicon continue to exhibit a broad variety of material properties that do not appear in silicon in its bulk form. Furthermore, this device is suitable for an optoelectronic integrated circuit environment and shows the possibility of realizing large-scale integrated silicon-based optoelectronic systems.

This work was supported in part by the National Science Foundation (DMI-0304650) and by the U.S. Army Research Office under MURI contract DAAD19-01-1-0603. C. J. Summers and T. Yamashita thank the Georgia Tech MiRC cleanroom staff for their valuable assistance. E. Schonbrun's e-mail address is Ethan.Schonbrun@colorado.edu.

References

1. S. G. Johnson, S. Fan, P. R. Villeneuve, J. D. Joannopoulos, and L. A. Kolodziejski, *Phys. Rev. B* **60**, 5751 (1999).
2. M. Loncar, D. Nedeljkovic, T. Doll, J. Vuckovic, A. Sherer, and T. P. Pearsall, *Appl. Phys. Lett.* **77**, 1937 (2000).
3. H. Kosaka, T. Kawashima, A. Tomita, M. Notomi, T. Tamamura, T. Sato, and S. Kawakami, *Appl. Phys. Lett.* **74**, 1212 (1999).
4. S. Shi, A. Sharkawy, C. Chen, D. Pustai, and D. Prather, *Opt. Lett.* **29**, 617 (2004).
5. E. Schonbrun, T. Yamashita, W. Park, and C. J. Summers, *Phys. Rev. B* **73**, 195117 (2006).
6. L. Wu, M. Mazilu, J. F. Gallet, T. F. Krauss, A. Jugessur, and R. M. De La Rue, *Opt. Lett.* **29**, 1620 (2004).
7. Y. Ohtera, T. Sato, T. Kawashima, T. Tamamura, and S. Kawakami, *Electron. Lett.* **35**, 1271 (1999).
8. S. Kim, G. P. Nordin, J. Cai, and J. Jiang, *Opt. Lett.* **28**, 2384 (2003).
9. S. G. Johnson and J. D. Joannopoulos, *Opt. Express* **8**, 173 (2001).
10. T. Yamashita and C. J. Summers, *IEEE J. Sel. Areas Commun.* **23**, 1341 (2005).